Non-Invasive Urodynamic Analysis Using the Computational Fluid Dynamics Method Based on MR Images

MR Görüntülerine Dayalı Hesaplamalı Akışkanlar Dinamiği Yöntemi ile Non-İnvazif Ürodinamik Analiz

Yusuf Z. ATEŞÇİ, MD,[a]
Utku ŞENTÜRK,[b]
Mahmut PEKEDİS,[b]
Murat ÇINAR[c]

[a]Clinic of Urology,
Şifa Hospital Group,
[b]Department of Mechanical Engineering,
Ege University Faculty of Engineering,
[c]Ege University
Nuclear Science Institute, İzmir

Yazışma Adresi/*Correspondence:*
Yusuf Z. ATEŞÇİ, MD
Şifa Hospital Group,
Clinic of Urology, İzmir,
TÜRKİYE/TURKEY
yatesci@yahoo.com

ABSTRACT Objective: The pressure-flow rate test is invasive. In addition, several nomograms are used and an exact standardization cannot be provided. For this reason, the search for new methods that are called non-invasive by several authorities, and that will provide clinical data similar to urodynamics, is ongoing. The aim of this study is to report a non-invasive, newly developed technique for the assessment of bladder pressure and flow rate using Computational Fluid Dynamics (CFD). **Material and Methods:** Participants consisted of 10 voluntary males. All data referring to volunteer demographics were recorded. Magnetic resonance imaging (MRI) was performed for the reconstruction of the bladder. After the MRI process, the peak flow-rates were measured with a uroflowmeter. Using CFD, first, by applying a pressure of 20 cm H_2O to the bladder wall the geometry of the bladder was obtained from processing of MR images and flow rates were determined. Secondly, the wall pressures needed to provide flow rates obtained from uroflowmetry were calculated. **Results:** The average values of the measured flow rate and the computed flow rate were calculated as 21.9 ± 7.8 ml/s and 24.6 ± 2.4 ml/s, respectively. It was found that the flow rates obtained from the uroflowmetry and the flow rates calculated by CFD were consistent with each other ($p < 0.05$). The average value of the computed bladder pressure was found to be 16.8 ± 9.6 cm H_2O. **Conclusion:** CFD, which is widely used in biomechanical applications as well as engineering problems, was used to simulate the flow inside three dimensional bladder models obtained from MR images. By comparing the results achieved by this method and the results obtained by uroflowmetry, a significant correlation was found. A novel non-invasive alternative method was developed to investigate the pressure-flow rate relationship in the bladder which may also provide a basis for theoretical analysis.

Key Words: Urodynamics; numerical analysis, computer-assisted; magnetic resonance imaging

ÖZET Amaç: Basınç-akım hızı testi invaziftir. Buna ek olarak bazı nomogramlar kullanılmakta ve tam bir standardizasyon sağlanamamaktadır. Bu sebeple, bazı otoriteler tarafından non-invazif olarak adlandırılan ve ürodinamiye benzer sonuçlar verecek arayışlar sürmektedir. Bu çalışmanın hedefi, mesane akım hızı ve basıncının belirlenmesi için Hesaplamalı Akışkanlar Dinamiği (HAD) kullanarak geliştirilen yeni bir tekniği sunmaktır. **Gereç ve Yöntemler:** Katılımcılar, 10 erkek gönüllüden oluşmuştur. Tüm katılımcı demografi verileri kaydedilmiştir. Mesanenin rekonstrüksiyonu için manyetik rezonans görüntüleme (MRG) uygulanmıştır. MRG işlemi ardından, üroflowmetri ile maksimum akım hızları ölçülmüştür. HAD kullanılarak, öncelikle, geometrisi MR görüntülerinin işlenmesi ile elde edilen mesanenin çeperine 20 cm H_2O uygulanarak akım hızları belirlenmiştir. İkinci olarak ise, üroflowmetriden elde edilen akım hızlarını sağlayacak çeper basınçları hesaplanmıştır. **Bulgular:** Ölçülen akım hızı ve hesaplanan akım hızının ortalama değerleri, sırasıyla, 21.9 ± 7.8 ml/s and 24.6 ± 2.4 ml/s'dir. Üroflowmetriden elde edilen ve HAD'dan hesaplanan akım hızları uyumlu olduğu görülmüştür ($p < 0.05$). Hesaplanan mesane basıncının ortalama değeri, 16.8 ± 9.6 cm H_2O bulunmuştur. **Sonuç:** Gerek mühendislik problemlerinde, gerekse biyomekanik uygulamalarında sıklıkla kullanılan HAD ile, MR görüntülerinden elde edilen üç boyutlu mesane modelleri içerisindeki akış simüle edilmiştir. Elde edilen sonuçlar, ürodinami sonuçları ile uyumludur. Mesane içerisindeki basınç-akım hızı ilişkisinin incelenmesinde, yeni, non-invazif ve alternatif bir yöntem geliştirilmiş olup, bu yöntem teorik analizlerde de bir temel oluşturabilir.

Anahtar Kelimeler: Ürodinamikler; sayısal analiz, bilgisayar-yardımlı; manyetik rezonans görüntüleme

Because urodynamic testing is difficult to implement and mostly invasive (needs catheterization, results are complicated and can be affected by artifacts), it is performed only for vital conditions in routine clinical applications. For instance, although the pressure-flow rate study is accepted as the gold standard examination for determination of the obstruction in lower urinary system, implementing this method on a patient for the decision of obstructive prostate surgery is not suggested in daily clinical application. This suggestion is not only because the pressure-flow rate test is invasive but also several nomograms are used and an exact standardization cannot be provided. For this reason, the search for new methods that are called non invasive by several authorities, and that will provide clinical data similar to urodynamics, is ongoing.[1-3]

Bladder outlet obstruction (BOO) is commonly associated with lower urinary tract symptoms (LUTS) in men.[4] BOO is a mechanical phenomenon; therefore, it is normally studied using mechanical parameters, such as pressure and flow. Urodynamic tests are the current standard for the classification of the degree of obstruction.[4] Pressure-flow studies constitute the gold standard for diagnosing BOO, through the use of the Abrams-Griffiths and Schäfer nomograms.[5,6]

This study aims to simulate the flow dynamics inside the bladder using Computational Fluid Dynamics (CFD) in order to develop an alternative non-invasive method to estimate the bladder pressure-urine flow rate relation. Here, only the peak value of the time dependent flow-rate curve is considered where the CFD procedure is combined with the reconstruction of three-dimensional bladder geometry using magnetic resonance (MR) images.

MATERIAL AND METHODS

In this study, a technique for the assessment of bladder pressure and urine flow rate using Computational Fluid Dynamics is investigated. This investigation has four stages. In the first stage, bladder images of subjects were scanned using magnetic resonance imaging (MRI). Three dimensional bladder models were constructed using these MR ima-

ges in the second stage. In the third stage, the urine flow inside the bladder was simulated using CFD. This stage had two steps: first, 20 cmH$_2$O pressure was implemented on the bladder walls and the average flow velocity at the proximal urethra was calculated. The second group of analyses included the investigation of the bladder wall pressure that will supply the clinically measured flow rate. In the fourth part, a statistical correlation between numerical and experimental data was determined.

PARTICIPANTS

The participants were 10 healthy, voluntary males. The participants had not undergone surgical treatment of the lower urinary tract and were not on medical treatment for their symptoms. This study follows the principles of the Helsinki Declaration.

PROCEDURE

MR imaging was carried out while the subjects were in the supine position with a full bladder. Siemens 1.5 Tesla closed MRI equipment was used. The subjects' images were examined on the bladders' sagittal and coronal plane with 1.5 mm cross-sections. After the MRI process, the urinary flow was measured with a Lifetech uroflowmeter. The clinical data can be seen in Table 1.

DATA ANALYSIS

To search for a correlation between the urinary flow and bladder pressure, 3D modeling of MR images of subjects' bladders and urinary system images were processed in three steps. A flowchart of the steps is given in Figure 1. These procedures are described stepwise in the following subchapters. The described software modules are not mandatory; however, during the development of this algorithm, we found no relevant issues in data transfer using these packages. The developed algorithm to generate an appropriate three dimensional model of the bladder (Figure 1) was based on a number of software packages used.

Image Processing

The MR images of the human bladder were obtained from different age and weight groups. Multi-

TABLE 1: Demographic data of volunteers.					
No	Age	Weight (kg)	Height (cm)	Body mass index	Waist circumference (cm)
1	33	72	178	22.72	92
2	30	78	174	25.76	102
3	25	71	162	27.05	96
4	48	82	168	29.06	128
5	55	92	180	28.39	106
6	29	90	175	29.38	105
7	46	80	174	26.42	121
8	22	70	160	27.34	90
9	31	75	172	25.35	104
10	28	84	173	28.06	95
	34.7±10.9	79.4±7.7	171.6±6.4	26.95±1.9	103.9±12.3

a) MR Scanning   **b)** MR surface construction   **c)** CFD
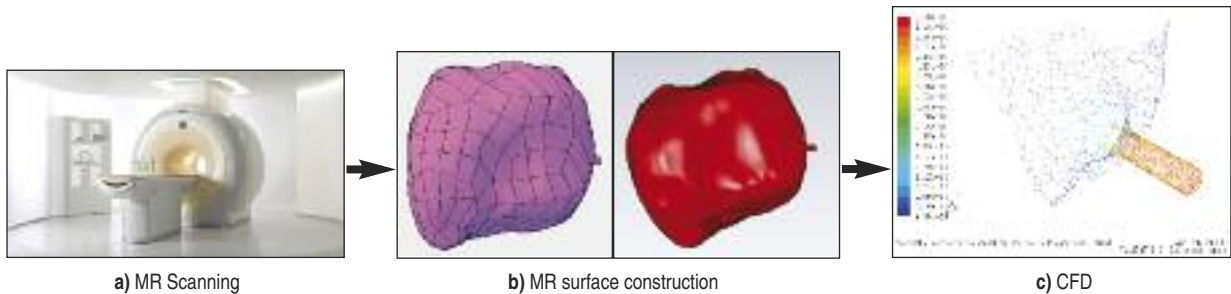
FIGURE 1: Basic steps of the implemented methodology: **a)** Obtaining the MR images of the human bladder, **b)** Implementation of three dimensional reconstruction and smoothing, **c)** CFD simulations.

MR: Magnetic resonance, CFD: Computational fluid dynamics.

ple cross sectional images of the bladder were scanned with an interval size of 1.5 mm using a Siemens MR device which is located at the Şifa Hospital, Izmir. Hospital, Therefore, the reconstruction of bladder morphology is based on a stack of MR-slices. The quality of the reconstructed bladder structures depends on the resolution and the voxel size of the MR-scan. During the imaging process, the participants were in the supine position. A total of 65 ± 4 images were taken. The files, which included all of the sectional slices calculated by the MRI scanner, were imported into the software MIMICS.

Three Dimensional Reconstruction of Bladder Morphology

First, the bladder region was identified, and then transferred to the reconstruction software. The surfaces of the model were constructed by identifying bladder and urethra regions. After the bladder configuration was labeled in all slices of the MRI scans, an automatic three dimensional reconstruction of the soft tissue was performed, creating triangulated surfaces. MIMICS provides tools to smooth the surface and to enhance its quality, but this can also be done in other software at a later stage.

For a clear formation of a three dimensional body out of the slices, it is important to remove holes and small islands in the labels. Corresponding functions for the removal of holes and islands are implemented in MIMICS. It might be necessary to adjust the position of the bladder in order to achieve a definite position. Finally, a smoother surface was achieved using AutoCAD software.

Computational Fluid Dynamics (CFD) Simulations of the Bladder

CFD is the process of obtaining approximate solutions to the Navier-Stokes equations which can be basically defined as the governing equations of

fluid motion, using numerical methods. Amongst several approaches, Finite Volume Method based on commercial code Fluent was used to discretise and solve these equations; as a result, the velocity and pressure fields inside the bladder were obtained.

In the preprocessing stage, the fluid domain was decomposed into a finite number of volumes by meshing the bladder geometries which were created from MR images. To investigate grid independency, each bladder model was meshed with three different resolutions (coarse, fine, very fine) and simulated. The mesh sizes for the highest mesh resolution are presented in Table 2.

In the analysis stage, the three dimensional flow inside the bladder was assumed to be incompressible, steady, turbulent. The boundary conditions are given in Figure 2. Trigon, which is the portion of the bladder that does not contribute to pressure, is also shown in Figure 2 as a wall type boundary.

The material properties are defined as the properties of water at 40°C having a density ρ=992 kg/m^3 and dynamic viscosity μ=0.657 × 10^{-3} kg/(ms). In the first group of analyses, 20 cm H$_2$O pressure was implemented on the bladder walls and the average of the flow velocity at the bladder outlet was calculated. The second group of analyses included the investigation of the bladder wall pressure that will supply the clinically measured flow rate of each case using the Target Mass Flow Rate feature of the software.

In the post processing stage, the pressure and the velocity fields were obtained. The area weighted average of the flow velocity and the volumetric flow rate of urine at the bladder outlet were calculated using Fluent.

Statistical Analysis

A non-parametric correlation test, the Spearman correlation, was used for the parameter selection.

TABLE 2: Computed flow rates at the proximal urethra at 20 cm H$_2$O bladder pressure.

No	Mesh Size	Flow Rate (ml/s)	
		Measured	Computed
1	1 121 131	41.1	25.9
2	634 376	21.2	25.7
3	489 637	18.0	27.2
4	1 015 206	17.7	23.6
5	1 131 954	15.9	21.6
6	470 952	28.7	25.8
7	1 155 723	23.3	25.8
8	460 226	18.9	27.8
9	471 325	19.4	21.5
10	356 420	15.1	21.6
	730695 ± 331730	21.9 ± 7.8	24.6 ± 2.4
			p= 0.028
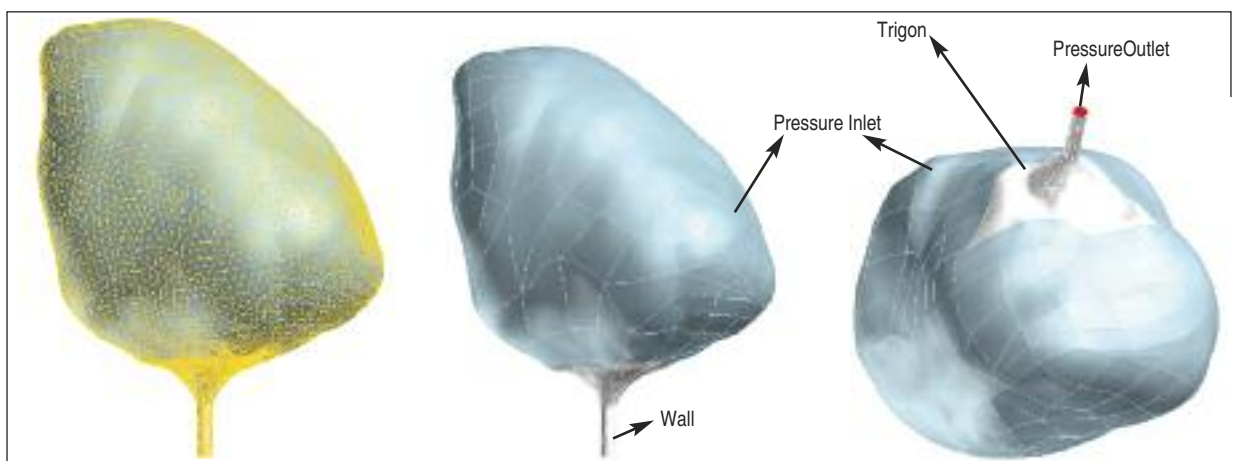
FIGURE 2: Three dimensivonal views and assigned boundary conditions for bladder no 1.

Statistical analyses were performed using the Statistical Package for Social Sciences (SPSS). A statistically significant level of p= 0.05 was used.

RESULTS

The velocity and pressure distributions that are obtained from CFD simulation of bladder no 1 are presented in Figure 3. Here, it is observed that urine maximum velocity occurs at the urethra-proximal urethra section. Additionally, the pressure distribution shown in Figure 3d states that the pressure decreases to minimum at the proximal urethra section as expected from Bernoulli's Theory.

In the first group of analyses, the flow rates at the proximal urethra were calculated from CFD simulations of 10 volunteers' bladders at 20 cm H_2O pressure since it is known that micturition pressure is approximately 20 cm H_2O clinically.[7] These values are presented in Table 2. In addition, peak values of measured flow rates are also given in Table 2 where the actual pressure inside the bladder may not necessarily be 20 cm H_2O. Thus, these flow rates are shown in order to investigate a possible correlation, rather than a direct comparison with each other. The p value in Table 2 belongs to the non-parametric Spearman correlation test. As a result, a positive correlation was found between the measured flow rate and computed flow rate, and this correlation was statistically significant (correlation coefficient= 0.689, p= 0.028< 0.05).

In the second group of analyses, the bladder pressure that will supply the peak flow rate from uroflowmetry is searched for each bladder model. For instance, the pressure within the bladder no 6 to provide the peak flow rate of 28.7 ml/s was found as 26.5 cm H_2O.

The results presented in Table 2 and 3 belong to the simulations of the highest mesh resolution. The effect of mesh resolution on the computed
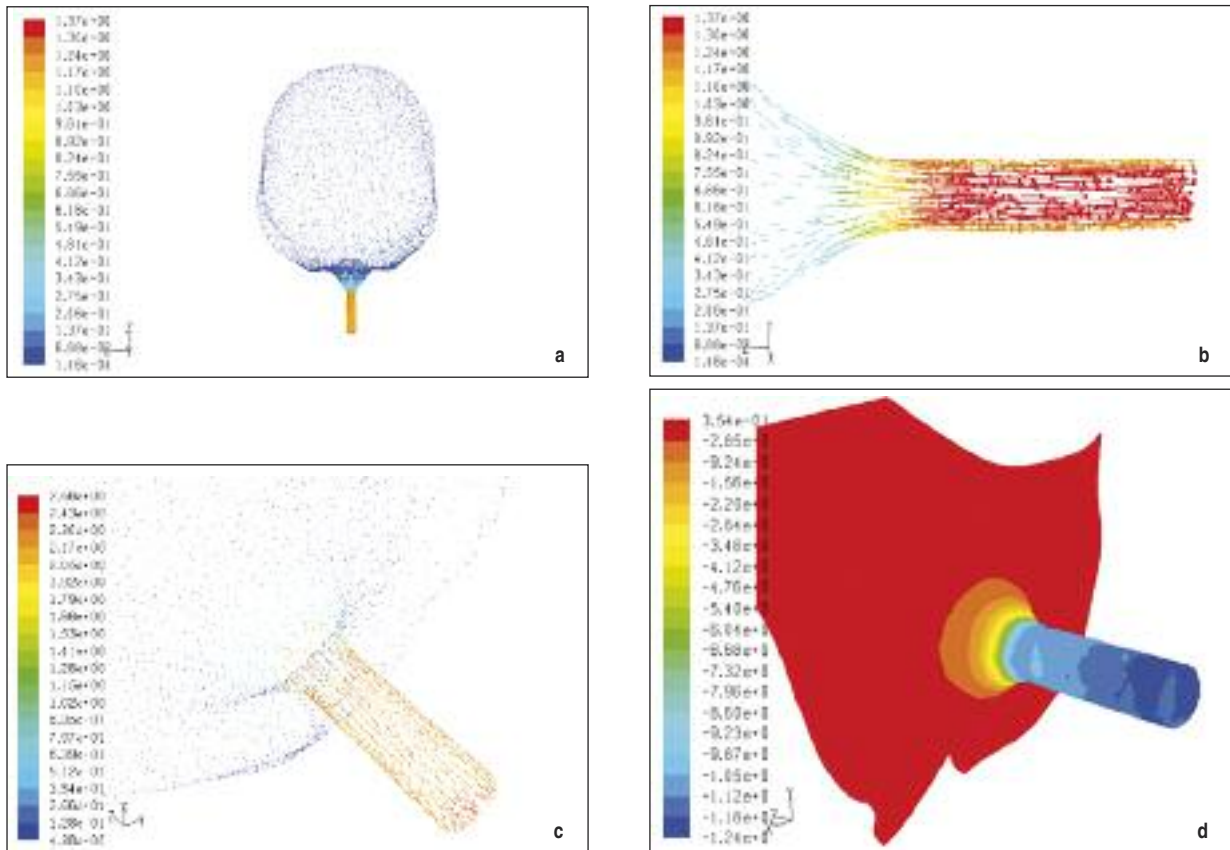
FIGURE 3: Numerical results obtained from CFD for bladder no 1: **a,b** and **c)** Several views of the velocity field **d)** pressure field.
CFD: Computational fluid dynamics.

flow rate is given in Table 4 as an example. Here, we concluded that by increasing mesh size, computed flow rate converges.

DISCUSSION

In recent years, there has been an increase of interest in non-invasive urodynamic techniques in an attempt to maximize diagnostic information before resorting to the invasive test with its costs and risks. For this reason, the search for new methods that are non-invasive is ongoing. Some of non-invasive urodynamics techniques devoloped in recent years are; the drop spectrometer,[8] Condom catheter,[9] Penile cuff deflation,[10] Penile cuff inflation,[11] Doppler ultrasound.[12]

Reis et al. measured the intravesical protrusion of the prostate (IPP) and prostatic volume through an abdominal ultrasound which is non invasive and accessible method that significantly correlated to urinary BOO, and they found it useful in the diagnosis of male urinary obstructive problems.[13]

Griffiths et al.[14] developed a new noninvasive test to measure bladder pressure in males based on controlled inflation of a penile cuff during voiding. They compared the new technique with simultaneous invasive bladder pressure measurement. They found that invasive and non-invasive pressure measurements agreed well. Average cuff pressure at interruption of flow exceeded mean simultaneous isovolumetric bladder pressure plus or minus standard deviation by 14.5 ± 14.0 cmH$_2$O. The average bladder pressure in our study was found to be 16.8 ± 9.6 cmH$_2$O which is in agreement with the results of Griffiths et al.

McArdle et al. assessed the variability in interpreting non invasive measurements of bladder pressure and urine flow between experienced and novice users of the bladder. They observed that excellent levels of agreement in measurement and categorization after a short training period suggested that introducing the penile cuff test as part of the assessment in men with lower urinary tract symptoms would be straightforward.[1] Clarkson et al. performed a pragmatic study of the penile cuff test; a noninvasive method of categorizing bladder outlet obstruction. They found that diagnostic category repeatability was similar to that of conventional urodynamics, although there was greater variability in pressure measurements.[2]

Stothers et al. reported a non invasive technique and numerical method of analysis for the assessment of BOO in male subjects using near-infrared spectroscopy (NIRS) and to test the independent ability of NIRS data to distinguish between patients with and without obstruction using a classification and regression tree algorithm. They found that using the classification and regression tree algorithm (CART) and non invasive NIRS data during voiding had an independent discriminatory ability related to the classification of BOO.[3]

Oelke et al. compared the diagnostic accuracy of detrusor wall thickness (DWT), free uroflowmetry, postvoiding residual urinary volume and prostate volume with pressure-flow studies to detect BOO in men. They reported that measure-

TABLE 3: Computed bladder wall pressure that will supply clinically measured flow rate.

No	Measured peak flow rate (ml/s)	Computed bladder pressure (cm H$_2$O)
1	41.1	40.6
2	21.2	13.5
3	18.0	10.8
4	17.7	13.2
5	15.9	10.6
6	28.7	26.5
7	23.3	16.6
8	18.9	11.1
9	19.4	14.9
10	15.1	10.4
	21.9 ± 7.8	16.8 ± 9.6

TABLE 4: Computed flow rates at 20 cm-H$_2$O bladder pressure for different mesh sizes (Bladder no 1).

Mesh size	Computed flow rate (ml/s)
149 507	27.3
527 696	26.05
1 121 131	25.9

ments of DWT could detect BOO better than free uroflowmetry, postvoiding residual urinary volume or prostate volume.[15]

McRae et al.[16] introduced the interesting idea of applying the principle of non-invasive blood pressure measurement to assess voiding pressure. They fitted a pediatric blood pressure cuff to the penis, inflated it and then, while the patient was trying to void, slowly deflated the cuff until flow began.

In a review by Griffiths and Pickard,[17] it has been stressed that Q_{max} > 15 ml/s is considered normal, Q_{max} < 10 ml/s is considered reduced for reasons of outlet obstruction or a weak bladder in men. Based on this criteria, we conclude that participants are considered normal (Table 2).

Jin et al.[18] developed a three-dimensional urodynamic bladder-urethra system, which includes bladder, bladder neck, prostate, and urethra; the realistic recirculation process of the urinary bladder during the physiologic voiding process in conjunction with a flow simulation through the female urinary bladder and urethra. They found that the computational results show that a dead-water zone and the zone of secondary flow occur, independent of the shape of the prostatic urethra. Pel and Mastrigt[19] developed a CFD urethral model including urethral geometry to study the relation between generated noise and the degree of obstruction. That model comprised a bladder, bladder neck, prostate and urethra. They found that the location of the maximum amplitude of perineal noise mainly depends on the degree and shape of the prostatic obstruction.

This study presents the implementation of CFD software widely used in engineering problems to bladder models obtained from MR images. In addition to the studies mentioned above,[18,19] the flow rate obtained from uroflowmetry was used as an input for CFD simulations. The results were then compared with the results of uroflowmetry.

In simulations, proximal urethral flow-rate was calculated assuming that the detrusor in the bladder contracted with a pressure of 20 cm H_2O. Via using this software on bladder simulations obtained from MR images, correlated results were found in terms of flow rates (Table 2).

Secondly, the bladder pressure to supply the peak flow rate which was acquired from uroflowmetry was calculated. It is known that micturition pressure is approximately 20 cm H_2O clinically.[8] The bladder pressure that will supply the clinically measured flow rate was found to be 16.8 ± 9.6 cm H_2O from CFD simulations (Table 3). When compared to the micturition pressure, this value indicates that present method yields valid results. It should be noted that lower pressure values are related to the neglected urethral and prosthatic resistances. When these parameters are taken into consideration by including urethra and prostate in the reconstruction process, an increased accuracy is expected. Additionally, insufficient contraction of patient detrusor is also another reason for low bladder pressure.

Urodynamics devices plot the patient's pressure-flow rate results on nomograms. The condition of the patient is then determined according to these nomograms. Most commonly referred nomograms are, Abrams-Griffiths Nomogram, Schafer Method, Group-Specific Urethral Resistance Factor Nomogram and the ICS Provisional Nomogram.[20] In practice, the comparison of the results of current study with these nomograms lead to confusion. For this reason, the simulations are based on the detrusor pressure at the maximum flow rate condition which eventually simplifies the evaluation of present method.

CONCLUSION

Conducted research that is presented in this paper is a preliminary study on urodynamics. It is foreseen that the use of the finite volume method with the Fluent software, together with sophisticated devices providing 3D images such as MR and ultrasound (no ionizing radiation), allows to obtain detailed information about the bladder without the need for invasive urodynamic techniques. The sig-

nificant correlation between simulation results and measured results show that the proposed model could be appropriate for bladder dynamics.

A comparative study of the current method with clinically measured pressure and flow rate data including the urethra and prostate anatomy will lead to standardization. Then, we believe that this method will serve as an alternative non-invasive method that could be used on behalf of urodynamics in the near future.

▌REFERENCES

1. McArdle F, Clarkson B, Robson W, Griffiths C, Drinnan M, Pickard R. Interobserver agreement for noninvasive bladder pressure flow recording with penile cuff. J Urol 2009;182(5):2397-403.

2. Clarkson B, Robson W, Griffiths C, McArdle F, Drinnan M, Pickard R. Multisite evaluation of noninvasive bladder pressure flow recording using the penile cuff device: assessment of test-retest agreement J Urol 2008;180(6):2515-21.

3. Stothers L, Guevara R, Macnab A. Classification of male lower urinary tract symptoms using mathematical modelling and a regression tree algorithm of noninvasive near-infrared spectroscopy parameters. Eur Urol 2010;57(2):327-32.

4. Nitti VW. Pressure flow urodynamic studies: the gold standard for diagnosing bladder outlet obstruction. Rev Urol 2005;7(Suppl 6):S14-21.

5. Abrams PH, Griffiths DJ. The assessment of prostatic obstruction from urodynamic measurements and from residual urine. Br J Urol 1979;51(2):129-34.

6. Schäfer W. Principles and clinical application of advanced urodynamic analysis of voiding function. Urol Clin North Am 1990;17(3):553-66.

7. Tanagho EA, Deng DY. Urodynamic studies. In: Tanagho EA, McAninch JW, eds. Smith's General Urology. 17th ed. Philadelphia: McGraw-Hill Medical; 2008. p.468-72.

8. Caffarel J, Griffiths C Pickard R, Robson W, Drinnan M. Modeling the clinical assessment of men with suspected obstructed voiding using bayes' theorem. Neurology and Urodynamics 2008;27(8):797-801.

9. Pel JJ, van Mastrigt R. Non-invasive measurement of bladder pressure using an external catheter. Neurourol Urodyn 1999;18(5):455-69.

10. Gleason DM, Bottaccini MR, McRae LP. Noninvasive urodynamics: a study of male voiding dysfunction. Neurourol Urodyn 1997;16(2):93-100.

11. Griffiths CJ, Rix D, MacDonald AM, Drinnan MJ, Pickard RS, Ramsden PD. Noninvasive measurement of bladder pressure by controlled inflation of a penile cuff. J Urol 2002;167(3):1344-7.

12. Belal M, Abrams P. Noninvasive methods of diagnosing bladder outlet obstruction in men. Part 2: Noninvasive urodynamics and combination of measures. J Urol 2006;176(1):29-35.

13. Reis LO, Barreiro GC, Baracat J, Prudente A, D'Ancona CA. Intravesical protrusion of the prostate as a predictive method of bladder outlet obstruction. Int Braz J Urol 2008;34(5):627-33.

14. Griffiths CJ, Rix D, MacDonald AM, Drinnan MJ, Pickard RS, Ramsden PD. Noninvasive measurement of bladder pressure by controlled inflation of a penile cuff. J Urol 2002;167(3):1344-7.

15. Oelke M, Höfner K, Jonas U, de la Rosette JJ, Ubbink DT, Wijkstra H. Diagnostic accuracy of noninvasive tests to evaluate bladder outlet obstruction in men: detrusor wall thickness, uroflowmetry, postvoid residual urine, and prostate volume. Eur Urol 2007;52(3):827-34.

16. McRae LP, Bottaccini MR, Gleason DM. Noninvasive quantitative method for measuring isovolumetric bladder pressure and urethral resistance in the male: I. Experimental validation of the theory. Neurourol Urodyn 1995;14(2):101-14.

17. Griffiths CJ, Pickard RS. Review of invasive urodynamics and progress towards non-invasive measurements in the assessment of bladder outlet obstruction. Indian J Urol 2009;25(1):83-91.

18. Jin Q, Zhang X, Li X, Wang J. Dynamics analysis of bladder-urethra system based on CFD. Front Mech Eng China 2010;5(3):336-40.

19. Pel JJ, van Mastrigt R. Development of a CFD urethral model to study flow-generated vortices under different conditions of prostatic obstruction. Physiol Meas 2007;28(1):13-23.

20. Campbell MF, Wein AJ, Kavoussi LR. Conducting the urodynamic evaluation. In: Wein AJ, Kavoussi LR, eds. Campbell-Walsh Urology. 9th ed. Philadelphia: WB Saunders; 2007. p.468-72.